

Finite volume evolution Galerkin methods for Euler equations of gas dynamics

M. Lukáčová-Medvid'ová¹ K. W. Morton² and G. Warnecke³

¹*Institute of Mathematics, University of Technology Brno, Czech Republic*

²*Oxford/Bath Universities, U.K.*

³*Institut für Analysis und Numerik, Otto-von-Guericke-Universität Magdeburg, Germany*

SUMMARY

The aim of this paper is a derivation of a new multidimensional high-resolution finite volume evolution Galerkin method for system of the Euler equations of gas dynamics. Instead of solving one-dimensional Riemann problems in directions normal to cell interfaces the finite volume evolution Galerkin schemes are based on a genuinely multidimensional approach. The approximate solution at cell interfaces is computed by means of an approximate evolution operator taking all of the infinitely many bicharacteristics explicitly into account. Integrals along the Mach cones are evaluated exactly or by means of numerical quadratures. Second-order resolution is obtained with a conservative piecewise bilinear recovery and the second-order midpoint rule for the time integration. A numerical experiment which illustrates the good multidimensional approximation as well as higher-order resolution is presented. Copyright © 2002 John Wiley & Sons, Ltd.

KEY WORDS: hyperbolic systems of conservation laws; Euler equations; genuinely multidimensional schemes; evolution Galerkin methods

1. INTRODUCTION

In recent years, the most commonly used methods for hyperbolic problems were finite volume methods which were based on a quasi-dimensional splitting using one-dimensional Riemann solvers. However, in multiple dimensions, there is in general no longer a finite number of directions of information propagation. Actually, it turned out that in certain cases, e.g. when waves are propagating in directions that are oblique with respect to the mesh, this approach leads to structural deficiencies and large errors in the solutions. Therefore, the emphasis has been put on developing genuinely multidimensional methods. In the 80s Deconinck *et al.* [1] presented the fluctuation splitting schemes. Each part of information, which is decomposed

* Correspondence to: M. Lukáčová-Medvid'ová, Institute of Mathematics, University of Technology Brno, Technická 2, Brno 61600, Czech Republic.

Contract/grant sponsor: Deutsche Forschungsgemeinschaft; contract/grant number: DFG/No. Wa 633/6-2

Contract/grant sponsor: Technical University Brno, contract/grant number: CZ 39001/2201, GACR 201/00/0557

Contract/grant sponsor: VolkswagenStiftung agency

into a discrete number of simple waves, is distributed in flow directions over the cell vertices. In 1997, LeVeque presented the wave propagation algorithm for multidimensional systems of conservation laws [3]. The scheme still works with a one-dimensional Riemann solver, however, it approximates not only the fluxes in x and y directions to cell interfaces, but also the cross-product fluxes. In the same time Fey developed the method of transport (MoT) for the Euler equations [2]. Fey's method is based on decomposing the Euler equations into a finite number of advection equations, and solving each of them separately by a multidimensional scheme. Further, Noelle introduced in Reference [10] the simplified version of MoT scheme using the so-called interfaced centered evolution.

The basic idea of the *evolution Galerkin scheme* (EG), introduced by Morton, is that transport quantities, which remain constant along the characteristic curves, are shifted and then projected onto a finite element space. It was Ostkamp [11] who first generalized EG schemes for multidimensional systems. In Reference [4] we have improved stability as well as accuracy of Ostkamp's original finite difference scheme. In References [5–7] new second-order finite difference EG schemes, as well as finite volume EG schemes, respectively, were derived and studied for the linear wave equation system.

The aim of this contribution is to present new multidimensional high-resolution finite volume evolution Galerkin methods for systems of non-linear hyperbolic conservation laws. We believe that the most satisfying methods for approximating evolutionary PDE's are based on approximating the corresponding evolutionary operator. In order to construct a genuinely multidimensional numerical scheme for hyperbolic conservation laws the exact integral equations are approximated by the approximate evolution operator in such a way that all of the infinitely many directions of propagation of bicharacteristics are explicitly taken into account. The finite volume evolution Galerkin methods are a genuine generalization of the original idea of Godunov using an evolution operator for a system in multidimensions. They combine the usually conflicting design objectives of using the conservation form and following the characteristics, or bicharacteristics. Instead of solving one-dimensional Riemann problems in normal directions to cell interfaces by some approximate Riemann solvers, we use a genuinely multidimensional approach. The approximate solution at cell interfaces is computed by means of an approximate evolution operator using bicharacteristics. This is a novel feature of our method.

2. EULER EQUATIONS AND THE EXACT INTEGRAL EQUATIONS

Consider the Euler equation system written in primitive variables

$$\mathbf{V}_t + \mathbb{A}_1(\mathbf{V})\mathbf{V}_x + \mathbb{A}_2(\mathbf{V})\mathbf{V}_y = 0, \quad \mathbf{x} = (x, y)^T \in \mathbb{R}^2 \quad (1)$$

where

$$\mathbf{V} := \begin{pmatrix} \rho \\ u \\ v \\ p \end{pmatrix}, \quad \mathbb{A}_1 := \begin{pmatrix} u & \rho & 0 & 0 \\ 0 & u & 0 & 1/\rho \\ 0 & 0 & u & 0 \\ 0 & \gamma p & 0 & u \end{pmatrix}, \quad \mathbb{A}_2 := \begin{pmatrix} v & 0 & \rho & 0 \\ 0 & v & 0 & 0 \\ 0 & 0 & v & 1/\rho \\ 0 & 0 & \gamma p & v \end{pmatrix}$$

Here ρ denotes the density, u and v components of velocities, p pressure and γ isentropic exponent. To derive integral equations we linearize system (1) by freezing the Jacobi matrices

at a suitable point $\tilde{P} = (\tilde{x}, \tilde{y}, \tilde{t})$. Denote by $\tilde{\mathbf{V}} = (\tilde{\rho}, \tilde{u}, \tilde{v}, \tilde{p})$ the local variables at the point \tilde{P} and by \tilde{c} the local speed of sound there, i.e. $\tilde{c} = \sqrt{\gamma \tilde{p}/\tilde{\rho}}$, where $\gamma = 1.4$ for dry air. Thus, the linearized system (1) with frozen constant coefficient has the form

$$\mathbf{V}_t + \mathbb{A}_1(\tilde{\mathbf{V}})\mathbf{V}_x + \mathbb{A}_2(\tilde{\mathbf{V}})\mathbf{V}_y = 0, \quad \mathbf{x} = (x, y)^T \in \mathbb{R}^2 \quad (2)$$

The eigenvalues of the matrix pencil $\mathbb{A}(\tilde{\mathbf{V}}) = \mathbb{A}_1(\tilde{\mathbf{V}})n_x + \mathbb{A}_2(\tilde{\mathbf{V}})n_y$, where $\mathbf{n} = \mathbf{n}(\theta) = (n_x, n_y)^T = (\cos \theta, \sin \theta)^T \in \mathbb{R}^2$ are

$$\lambda_1 = \tilde{u} \cos \theta + \tilde{v} \sin \theta - \tilde{c}, \quad \lambda_2 = \lambda_3 = \tilde{u} \cos \theta + \tilde{v} \sin \theta, \quad \lambda_4 = \tilde{u} \cos \theta + \tilde{v} \sin \theta + \tilde{c} \quad (3)$$

and the corresponding linearly independent right eigenvectors are

$$\mathbf{r}_1 = \begin{pmatrix} -\tilde{\rho}/\tilde{c} \\ \cos \theta \\ \sin \theta \\ -\tilde{\rho}\tilde{c} \end{pmatrix}, \quad \mathbf{r}_2 = \begin{pmatrix} 1 \\ 0 \\ 0 \\ 0 \end{pmatrix}, \quad \mathbf{r}_3 = \begin{pmatrix} 0 \\ \sin \theta \\ -\cos \theta \\ 0 \end{pmatrix}, \quad \mathbf{r}_4 = \begin{pmatrix} \tilde{\rho}/\tilde{c} \\ \cos \theta \\ \sin \theta \\ \tilde{\rho}\tilde{c} \end{pmatrix}$$

Let $\mathbb{R}(\tilde{\mathbf{V}})$ be the matrix of the right eigenvectors. The inverse of $\mathbb{R}(\tilde{\mathbf{V}})$ is

$$\mathbb{R}^{-1}(\tilde{\mathbf{V}}) = \frac{1}{2} \begin{pmatrix} 0 & \cos \theta & \sin \theta & -1/(2\tilde{\rho}\tilde{c}) \\ 1 & 0 & 0 & -1/\tilde{c}^2 \\ 0 & \sin \theta & -\cos \theta & 0 \\ 0 & \cos \theta & \sin \theta & 1/(2\tilde{\rho}\tilde{c}) \end{pmatrix}$$

Multiplying system (2) by $\mathbb{R}^{-1}(\tilde{\mathbf{V}})$ from the left we obtain the characteristic system

$$\mathbf{W}_t + \mathbb{B}_1(\tilde{\mathbf{V}})\mathbf{W}_x + \mathbb{B}_2(\tilde{\mathbf{V}})\mathbf{W}_y = 0$$

where

$$\mathbb{B}_1 = \begin{pmatrix} \tilde{u} - \tilde{c} \cos \theta & 0 & -\frac{1}{2}\tilde{c} \sin \theta & 0 \\ 0 & \tilde{u} & 0 & 0 \\ -\tilde{c} \sin \theta & 0 & \tilde{u} & \tilde{c} \sin \theta \\ 0 & 0 & \frac{1}{2}\tilde{c} \sin \theta & \tilde{u} + \tilde{c} \cos \theta \end{pmatrix} \quad (4)$$

$$\mathbb{B}_2 = \begin{pmatrix} \tilde{v} - \tilde{c} \sin \theta & 0 & \frac{1}{2}\tilde{c} \cos \theta & 0 \\ 0 & \tilde{v} & 0 & 0 \\ \tilde{c} \cos \theta & 0 & \tilde{v} & -\tilde{c} \cos \theta \\ 0 & 0 & -\frac{1}{2}\tilde{c} \cos \theta & \tilde{v} + \tilde{c} \sin \theta \end{pmatrix}$$

and the characteristic variables \mathbf{W} are

$$\mathbf{W} = \begin{pmatrix} w_1 \\ w_2 \\ w_3 \\ w_4 \end{pmatrix} = \mathbb{R}^{-1}(\tilde{\mathbf{V}})\mathbf{V} = \begin{pmatrix} \frac{1}{2}(-p/\tilde{\rho}\tilde{c} + u \cos \theta + v \sin \theta) \\ \rho - p/\tilde{c}^2 \\ u \sin \theta - v \cos \theta \\ \frac{1}{2}(p/\tilde{\rho}\tilde{c} + u \cos \theta + v \sin \theta) \end{pmatrix} \quad (5)$$

The quasi-diagonalized system of the linearized Euler equations has the following form:

$$\begin{aligned} \mathbf{W}_t + \begin{pmatrix} \tilde{u} - \tilde{c} \cos \theta & 0 & 0 & 0 \\ 0 & \tilde{u} & 0 & 0 \\ 0 & 0 & \tilde{u} & 0 \\ 0 & 0 & 0 & \tilde{u} + \tilde{c} \cos \theta \end{pmatrix} \mathbf{W}_x \\ + \begin{pmatrix} \tilde{v} - \tilde{c} \sin \theta & 0 & 0 & 0 \\ 0 & \tilde{v} & 0 & 0 \\ 0 & 0 & \tilde{v} & 0 \\ 0 & 0 & 0 & \tilde{v} + \tilde{c} \sin \theta \end{pmatrix} \mathbf{W}_y = \mathbf{S} \end{aligned} \tag{6}$$

with

$$\mathbf{S} = \begin{pmatrix} S_1 \\ S_2 \\ S_3 \\ S_4 \end{pmatrix} = \begin{pmatrix} \frac{1}{2} \tilde{c} (\sin \theta \partial w_3 / \partial x - \cos \theta \partial w_3 / \partial y) \\ 0 \\ \tilde{c} \sin \theta (\partial w_1 / \partial x - \partial w_4 / \partial x) - \tilde{c} \cos \theta (\partial w_1 / \partial y - \partial w_4 / \partial y) \\ \frac{1}{2} \tilde{c} (-\sin \theta \partial w_3 / \partial x + \cos \theta \partial w_3 / \partial y) \end{pmatrix}$$

In what follows we will work with the concept of bicharacteristics. The ℓ th bicharacteristic \mathbf{x}_ℓ corresponding to the ℓ th equation of the system (2) is defined by

$$\frac{d\mathbf{x}_\ell}{dt} = \mathbf{b}_{\ell\ell}(\mathbf{n}) := (b_{\ell\ell}^1, b_{\ell\ell}^2)^T \tag{7}$$

where $B_1 = (b_{jk}^1)_{1 \leq j,k \leq 4}$, $B_2 = (b_{jk}^2)_{1 \leq j,k \leq 4}$. The set of all bicharacteristics creates the so-called Mach cone. We integrate the ℓ th equation of system (2) from the apex $P = (x, y, t + \Delta t)$ down to the footprint $Q_\ell(\theta)$. More precisely, the footprints of the corresponding bicharacteristics are

$$\begin{aligned} Q_1(\theta) &= (x - (\tilde{u} - \tilde{c} \cos \theta)\Delta t, y - (\tilde{v} - \tilde{c} \sin \theta)\Delta t, t) \\ Q_2 &= Q_3 = (x - \tilde{u}\Delta t, y - \tilde{v}\Delta t, t) \\ Q_4(\theta) &= (x - (\tilde{u} + \tilde{c} \cos \theta)\Delta t, y - (\tilde{v} + \tilde{c} \sin \theta)\Delta t, t) \end{aligned}$$

Integration of system (6) along the bicharacteristics gives the relations for the characteristics variables, which after the multiplication from the left by the matrix \mathbb{R} yield the exact integral equation. After some computation, see Reference [9], we get the exact integral equations for the Euler equations. Note that due to a symmetry between the points Q_1 and Q_4 we can express the following integral equations using only one of them

$$\rho(P) = \rho(Q_2) - \frac{p(Q_2)}{\tilde{c}^2} + \frac{1}{2\pi} \int_0^{2\pi} \left[\frac{p(Q_1)}{\tilde{c}^2} - \frac{\tilde{\rho}}{\tilde{c}} u(Q_1) \cos \theta - \frac{\tilde{\rho}}{\tilde{c}} v(Q_1) \sin \theta \right] d\theta$$

$$-\frac{\tilde{\rho}}{\tilde{c}} \frac{1}{2\pi} \int_0^{2\pi} \int_t^{t+\Delta t} S(\mathbf{x} - (\tilde{\mathbf{u}} - c\mathbf{n}(\theta))(t + \Delta t - \tilde{t}), \tilde{t}, \theta) d\tilde{t} d\theta, \quad (8)$$

$$\begin{aligned} u(P) &= \frac{1}{2\pi} \int_0^{2\pi} \left[-\frac{p(Q_1)}{\tilde{\rho}\tilde{c}} \cos \theta + u(Q_1) \cos^2 \theta + v(Q_1) \sin \theta \cos \theta \right] d\theta \\ &+ \frac{1}{2\pi} \int_0^{2\pi} \int_t^{t+\Delta t} \cos \theta S(\mathbf{x} - (\tilde{\mathbf{u}} - c\mathbf{n}(\theta))(t + \Delta t - \tilde{t}), \tilde{t}, \theta) d\tilde{t} d\theta \\ &+ \frac{1}{2} u(Q_2) - \frac{1}{2\tilde{\rho}} \int_t^{t+\Delta t} p_x(Q_2(\tilde{t})) d\tilde{t}, \end{aligned} \quad (9)$$

$$\begin{aligned} v(P) &= \frac{1}{2\pi} \int_0^{2\pi} \left[-\frac{p(Q_1)}{\tilde{\rho}\tilde{c}} \sin \theta + u(Q_1) \cos \theta \sin \theta + v(Q_1) \sin^2 \theta \right] d\theta \\ &+ \frac{1}{2\pi} \int_0^{2\pi} \int_t^{t+\Delta t} \sin \theta S(\mathbf{x} - (\tilde{\mathbf{u}} - c\mathbf{n}(\theta))(t + \Delta t - \tilde{t}), \tilde{t}, \theta) d\tilde{t} d\theta \\ &+ \frac{1}{2} v(Q_2) - \frac{1}{2\tilde{\rho}} \int_t^{t+\Delta t} p_y(Q_2(\tilde{t})) d\tilde{t}, \end{aligned} \quad (10)$$

$$\begin{aligned} p(P) &= \frac{1}{2\pi} \int_0^{2\pi} [p(Q_1) - \tilde{\rho}\tilde{c}u(Q_1) \cos \theta - \tilde{\rho}\tilde{c}v(Q_1) \sin \theta] d\theta \\ &- \tilde{\rho}\tilde{c} \frac{1}{2\pi} \int_0^{2\pi} \int_t^{t+\Delta t} S(\mathbf{x} - (\tilde{\mathbf{u}} - c\mathbf{n}(\theta))(t + \Delta t - \tilde{t}), \tilde{t}, \theta) d\tilde{t} d\theta \end{aligned} \quad (11)$$

where $(\mathbf{x} - (\tilde{\mathbf{u}} - c\mathbf{n}(\theta))(t + \Delta t - \tilde{t})) = (x - (\tilde{u} - \tilde{c} \cos \theta)(t + \Delta t - \tilde{t}), y - (\tilde{v} - \tilde{c} \sin \theta)(t + \Delta t - \tilde{t}))$, and the so-called source term S is given in the following form:

$$S(\mathbf{x}, t, \theta) := \tilde{c}[u_x(\mathbf{x}, t, \theta) \sin^2 \theta - (u_y(\mathbf{x}, t, \theta) + v_x(\mathbf{x}, t, \theta)) \sin \theta \cos \theta + v_y(\mathbf{x}, t, \theta) \cos^2 \theta]$$

3. APPROXIMATE EVOLUTION OPERATOR

Analogously as for the wave equation system in Reference [4] the integrals of the source term with respect to time will be approximated by the rectangle rule. Therefore, we would need to evaluate derivatives of the velocity components at time t . However, we found in Reference [4, Lemma 2.1], that the integrals of the source S can be simplified through integration by parts, which yields

$$\Delta t \int_0^{2\pi} S(t, \theta) d\theta = \int_0^{2\pi} [u_{Q_1} \cos \theta + v_{Q_1} \sin \theta] d\theta \quad (12)$$

Analogous relations hold for the $S \sin(\theta)$ and $S \cos(\theta)$ terms. The integrals in (9) and (10) involving p_x and p_y need to be replaced by integrals over the cone mantle. This is done by using the Gauss theorem, see Reference [4]. In such a way we have generated an approximate

evolution operator

$$\begin{aligned} \rho(P) = & \rho(Q_2) - \frac{p(Q_2)}{\tilde{c}^2} + \frac{1}{2\pi} \int_0^{2\pi} \frac{p(Q_1)}{\tilde{c}^2} - 2\frac{\tilde{\rho}}{\tilde{c}} u(Q_1) \cos \theta \\ & - 2\frac{\tilde{\rho}}{\tilde{c}} v(Q_1) \sin \theta \, d\theta + O(\Delta t^2) \end{aligned} \quad (13)$$

$$\begin{aligned} u(P) = & \frac{1}{2}u(Q_2) + \frac{1}{2\pi} \int_0^{2\pi} -\frac{2}{\tilde{\rho}\tilde{c}} p(Q_1) \cos \theta + u(Q_1)(3 \cos^2 \theta - 1) \\ & + 3v(Q_1) \sin \theta \cos \theta \, d\theta + O(\Delta t^2) \end{aligned} \quad (14)$$

$$\begin{aligned} v(P) = & \frac{1}{2}v(Q_2) + \frac{1}{2\pi} \int_0^{2\pi} -\frac{2}{\tilde{\rho}\tilde{c}} p(Q_1) \sin \theta + 3u(Q_1) \sin \theta \cos \theta \\ & + v(Q_1)(3 \sin^2 \theta - 1) \, d\theta + O(\Delta t^2) \end{aligned} \quad (15)$$

$$p(P) = \frac{1}{2\pi} \int_0^{2\pi} p(Q_1) - 2\tilde{\rho}\tilde{c}u(Q_1) \cos \theta - 2\tilde{\rho}\tilde{c}v(Q_1) \sin \theta \, d\theta + O(\Delta t^2) \quad (16)$$

where $Q_1 = (x - \Delta t(\tilde{u} - \tilde{c} \cos \theta), y - \Delta t(\tilde{v} - \tilde{c} \sin \theta), t)$, $Q_2 = (x - \Delta t\tilde{u}, y - \Delta t\tilde{v}, t)$, and $P = (x, y, t + \Delta t)$.

4. FINITE VOLUME EVOLUTION GALERKIN METHOD

In order to derive the finite volume EG schemes let us consider the Euler equations in the conservation form:

$$\mathbf{U}_t + \mathbf{F}_1(\mathbf{U})_x + \mathbf{F}_2(\mathbf{U})_y = 0 \quad (17)$$

where the vector of conservative variables and the fluxes are

$$\mathbf{U} := \begin{pmatrix} \rho \\ \rho u \\ \rho v \\ e \end{pmatrix}, \quad \mathbf{F}_1(\mathbf{U}) := \begin{pmatrix} \rho u \\ \rho u^2 + p \\ \rho uv \\ (e + p)u \end{pmatrix}, \quad \mathbf{F}_2(\mathbf{U}) := \begin{pmatrix} \rho v \\ \rho uv \\ \rho v^2 + p \\ (e + p)v \end{pmatrix}.$$

Here e stands for the total energy, i.e. $e = p/(\gamma - 1) + \rho(u^2 + v^2)/2$.

The finite volume EG methods works with the above conservation form of the Euler equations. However, instead of computing one-dimensional Riemann problems in the normal direction to cell interfaces by some approximate Riemann solver, we use multidimensional approach. The approximate solution at cell interfaces is computed by means of the approximate evolution operator using bicharacteristics, which works with the primitive variables, see (13)–(16).

If no recovery is used then the whole method is of first order. In this case the finite volume evolution Galerkin scheme reads

$$\mathbf{U}^{n+1} = \mathbf{U}^n - \frac{\Delta t}{h} \sum_{k=1}^2 \delta_{x_k} \mathbf{F}_k(\mathbf{U}^*) \quad (18)$$

$$\mathbf{F}_k(\mathbf{U}^*) = \frac{1}{h} \int_0^h F_k(E_{\Delta t/2} \mathbf{V}^n) d\ell \quad (19)$$

However, the most important advantage of the finite volume formulation is that even a first-order accurate approximation E_τ to the exact integral Equations (8)–(11) yields an overall second-order update from \mathbf{U}^n to \mathbf{U}^{n+1} . A second-order scheme is obtained by a conservative discontinuous bilinear recovery R_h using vertex values, and by the midpoint rule for time integration. Thus the fluxes on cell interface are computed as

$$\mathbf{F}_k(\mathbf{U}^*) = \frac{1}{h} \int_0^h F_k(E_{\Delta t/2} R_h \mathbf{V}^n) d\ell \quad (20)$$

We have applied the above FVEG methods very successfully to linear systems, e.g. the wave equation system, the Maxwell equations. In References [5, 6] we presented several results of numerical experiments and showed that the above approach led to relatively very accurate schemes. For example, in comparison with the Lax–Wendroff scheme (rotated-Richtmyer version) the second-order FVEG1 method is 7 times more accurate, see Reference [6]. For linear problems the EG-methods capture multidimensional effects like rotational symmetry, circular shocks and preservation of vorticity very well, see References [4–6].

Now, in order to compute *non-linear* fluxes on cell interfaces by means of the approximate evolution operator we need to define the local velocities of the flow (\tilde{u}, \tilde{v}) as well as the local speed of sound \tilde{c} . Therefore to construct local Mach cones it is suitable to put predicted points \tilde{P} on cell boundaries, e.g. at vertices or at midpoints of the edges. It can be shown, see Reference [9], that taking $\tilde{t} = t_n$ a linearization error is of order $\mathcal{O}(\Delta t)$, while $\tilde{t} = t_n + \Delta t/2$ leads to the second-order linearization error $\mathcal{O}(\Delta t^2)$. Now being at time t_n we have no information about the solution at time $t_n + \Delta t/2$. Therefore, a predictor step is needed to compute solution at $t_n + \Delta t/2$. In our computations we have used the Lax–Friedrichs or the Osher–Solomon method to compute this auxiliary information.

5. NUMERICAL RESULTS

Consider the well-known Sod-2d test problem with the initial data

$$\begin{aligned} \rho = 1, \quad u = 0, \quad v = 0, \quad p = 1, \quad \|\mathbf{x}\| < 0.4 \\ \rho = 0.125, \quad u = 0, \quad v = 0, \quad p = 0.1, \quad \text{else.} \end{aligned}$$

This initial-value problem may be considered as a spherical explosion problem. The computational domain is a square $[-1, 1] \times [-1, 1]$. The mesh is quadrilateral and initial data are

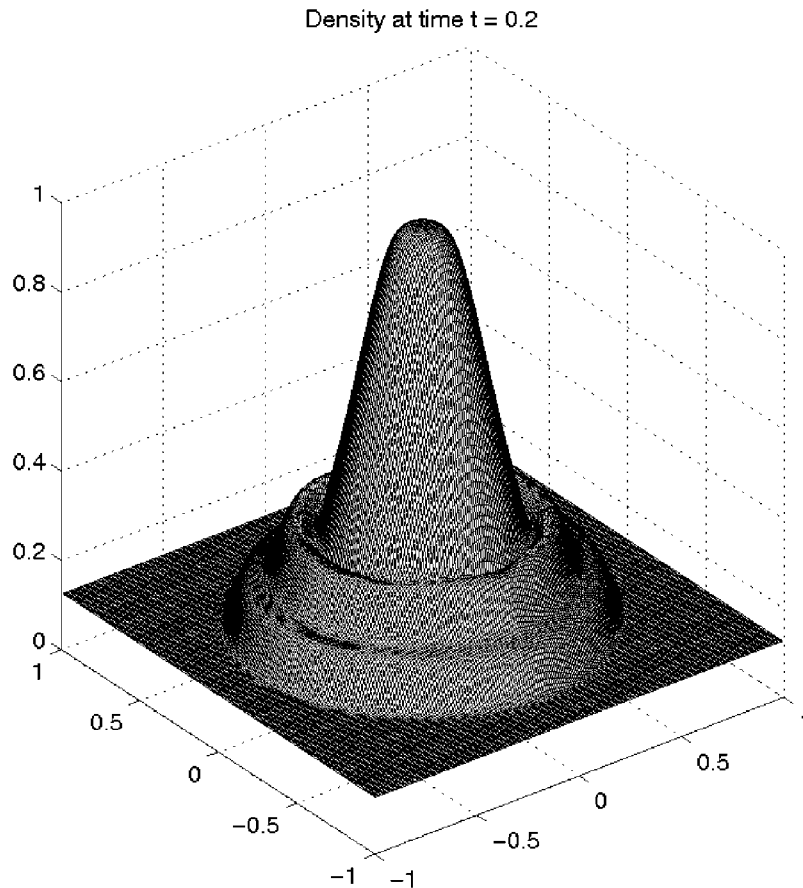


Figure 1. Cylindrical explosion, density distribution at $T = 0.2$ on a 200×200 mesh.

implemented by cutting the initial discontinuity and assigning it by modified area-weighted values according to the corresponding cell. As pointed out by Toro in Reference [12] this avoids the formation of small amplitude waves created at early times by staircase configuration of the data. We set the CFL number to 0.55. Note that the approximate evolution operator (13)–(16) leads to the FVEG scheme, which is not stable up to $\text{CFL} = 1$, but in Reference [8] a new FVEG scheme is derived, which is stable up to $\text{CFL} = 1$.

Figure 1 shows the density distribution as a function of x and y at time $T = 0.2$. The solution exhibits a circular shock travelling away from the centre, a circular contact discontinuity travelling in the same direction and a circular rarefaction wave travelling towards the origin at $(0, 0)$. In Figure 2 the isolines of density, x -velocity, and pressure are depicted.

In order to get more information on the exact solution we solved the one-dimensional non-homogeneous cylindrically symmetric Euler equations using the finite volume method of Roe on a fine mesh. Figure 3 shows the comparison between the ‘exact’ solution obtained by the one-dimensional FVM and the first as well as the second-order FVEG methods. We can

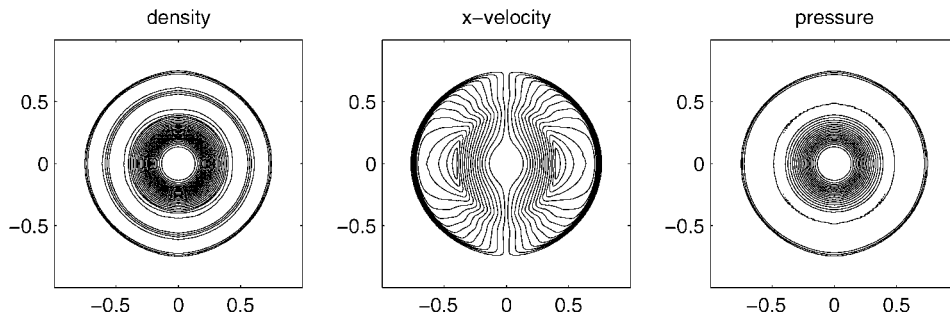


Figure 2. Isolines of the solution obtained by the FVEG scheme on a 400×400 mesh.

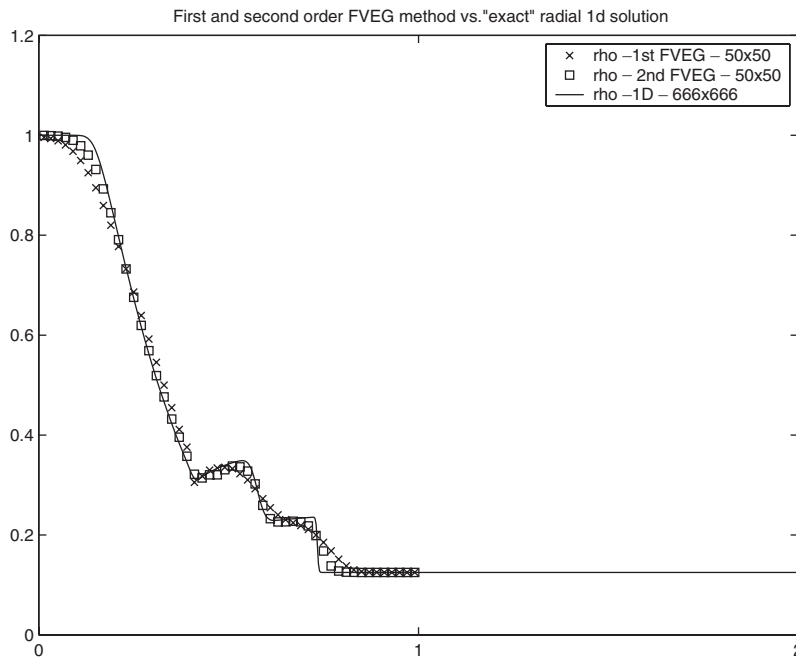


Figure 3. Comparison between the one-dimensional cylindrically symmetric solution and first as well as second-order FVEG methods.

notice that the second-order method resolves discontinuities more sharply and approximates the maxima of the solution more accurately.

ACKNOWLEDGEMENTS

The present research has been supported under the DFG Grant No. Wa 633/6-2 of Deutsche Forschungsgemeinschaft, by the Grants GACR 201/00/0557 and CZ 39001/2201 of the Technical

University Brno, as well as by the VolkswagenStiftung Grant Agency. The authors gratefully acknowledge these supports.

REFERENCES

1. Deconinck H, Struijs R, Roe P. Fluctuation splitting schemes for the 2D Euler equations. *Report 1991-11/AR*, Von Karman Institute, Belgium, 1991.
2. Fey M. Multidimensional upwinding, Part II. Decomposition of the Euler equations into advection equations. *Journal of Computational Physics* 1998; **143**:181–199.
3. LeVeque RJ. Wave propagation algorithms for multi-dimensional hyperbolic systems. *Journal of Computational Physics* 1997; **131**:327–353.
4. Lukáčová-Medvid'ová M, Morton KW, Warnecke G. Evolution Galerkin methods for hyperbolic systems in two space dimensions. *Mathematics of Computation* 2000; **69**:1355–1384.
5. Lukáčová-Medvid'ová M, Morton KW, Warnecke G. Finite volume evolution Galerkin methods for multidimensional hyperbolic problems, In Vilsmeier R *et al.* (eds), *Proceedings of the Finite Volumes for Complex Applications* Hermès: 1999; 289–296.
6. Lukáčová-Medvid'ová M, Morton KW, Warnecke G. High-resolution finite volume evolution Galerkin schemes for multidimensional conservation laws. *Proceedings of ENUMATH'99*. World Scientific Publishing Company: Singapore, 1999.
7. Lukáčová-Medvid'ová M, Warnecke G. Lax–Wendroff type second order evolution Galerkin methods for multidimensional hyperbolic systems. *East-West Journal of Numerical Analysis* 2000; **8**(2):127–152.
8. Lukáčová-Medvid'ová M, Morton KW, Warnecke G. Finite volume evolution Galerkin methods for hyperbolic systems, *in preparation*.
9. Lukáčová-Medvid'ová M, Saibertová J, Warnecke G. Finite volume evolution Galerkin methods for nonlinear hyperbolic systems. *Journal of Computational Physics* 2002, submitted.
10. Noelle S. The MOT-ICE: a new high-resolution wave-propagation algorithm for multi-dimensional systems of conservative laws based on Fey's method of transport. *Journal of Computational Physics* 2000; **164**:283–334.
11. Ostkamp S. Multidimensional characteristic Galerkin schemes and evolution operators for hyperbolic systems. *Mathematical Methods in the Applied Sciences* 1997; **20**:1111–1125.
12. Toro EF. *Riemann Solvers and Numerical Methods for Fluid Dynamics, A Practical Introduction*. Springer: Berlin, 1999.